Diameter-Dependent Band Gap Modification of Single-Walled Carbon Nanotubes by Encapsulated Fullerenes

Shingo Okubo,[†,||] Toshiya Okazaki,*[,†,‡] Naoki Kishi,[†,⊥] Soon-Kil Joung,[†] Takeshi Nakanishi,[†] Susumu Okada,[§] and Sumio Iijima[†]

Research Center for Advanced Carbon Materials, National Institute of Advanced Industrial Science and Technology, Tsukuba 305-8565, Japan, PRESTO, Japan Science and Technology Agency, 4-1-8 Honcho, Kawaguchi 332-0012, Japan, Institute of Physics and Center for Computational Sciences, University of Tsukuba, 1-1-1 Tennodai, Tsukuba 305-8577, Japan, and CREST, Japan Science and Technology Agency, 4-1-8 Honcho, Kawaguchi 332-0012, Japan

Received: August 27, 2008; Revised Manuscript Received: November 10, 2008

Band gap photoluminescence (PL) of single-walled carbon nanotubes (SWCNTs) encapsulating C_{60} fullerenes (nanopeapods) is examined over a wide range of diameters (~1.25−1.55 nm). The encapsulated fullerenes induce characteristic PL peak shifts that strongly depend on the tube diameter (d_t) and the "$2n + m$" family type {type I [mod($2n + m$, 3) = 1] and type II [mod($2n + m$, 3) = 2]}. This behavior can be explained by the strain-induced band gap shifts due to the C_{60} insertion and the hybridization between the electronic states of SWCNTs and C_{60}. The present results provide significant insights into band gap engineering of SWCNTs in future nanodevices.

Introduction

Because of their tubular structures, single-walled carbon nanotubes (SWCNTs) have been demonstrated to encapsulate various molecules and atoms.[1,2] The mechanical, electronic, and transport properties of SWCNTs frequently undergo considerable modification upon encapsulation, which allow us to finely tune these parameters by altering the encapsulated species. For example, fullerenes can be inserted in SWCNTs to form a linear chain of molecules, so-called nanopeapods.[2] Low-temperature scanning tunneling spectroscopy (LT-STS) revealed that a band gap of semiconducting SWCNTs is narrowed at the site where fullerene molecules reside.[3] Such band gap modulation leads to a substantial change in transport properties of SWCNTs. Actually, the *p*-type field-effect transistor (FET) behavior of SWCNTs was changed to be ambipolar by insertion of fullerenes.[4]

On the other hand, discovery of photoluminescence (PL) of SWCNTs has paved the new way for investigating their unique electronic properties associated with band gap structures.[5] The origin of the observed PL peak was reliably assigned to SWCNTs with specific chiral indexes (n, m) because the emission and excitation spectra show characteristic peaks, depending on the molecular structure of SWCNTs. Therefore, the PL method can provide rich information about electronic properties for individual (n, m) nanotubes at a resolution of a few millielectron volts.

Recently, optical band gap modifications of SWCNTs by encapsulated fullerenes were reported by using photoluminescence excitation (PLE) spectroscopy.[6] One of the important factors for band gap modification is found to be a diameter of SWCNTs because the interaction between the host SWCNTs and the guest C_{60} is sensitive to the interwall distance. For further characterization of the tube−fullerene interactions, however, investigations of various types of nanopeapods are needed. Especially, SWCNTs having larger diameters should be examined to elucidate the detailed mechanisms of the band gap change. In the previous report, SWCNTs produced by the pulsed-laser vaporization (PLV) method were used for the templates of nanopeapods.[6] The diameter of PLV-SWCNTs ranges from 1.2 to 1.4 nm.[7]

The SWCNTs produced by the arc-discharging method are suited for this purpose because the diameter of arc SWCNTs is normally larger than those of PLV-SWCNTs ($d_t \approx 1.3-1.5$ nm). However, it is well-known that arc SWCNTs contain substantial amounts of impurities such as amorphous carbons that severely decrease the filling yield. To overcome this problem, we have developed an effective purification method which incorporates an alkaline alcohol treatment. The effective purification drastically enhances the filling yield, which allows us to investigate the electronic properties in detail by the PLE measurements. In particular, the PL peaks from eight (n, m) nanopeapods with $d_t > 1.4$ nm are newly identified in the present study. Consequently, the present results combined with those obtained in the previous PLE studies[6] provide significant insights into the basic mechanism of band gap modification of nanopeapods. The change in the SWCNT band gap can be attributed to the mechanical strain by the encapsulated C_{60} or the hybridization between the electronic states of C_{60} and SWCNTs, depending on the tube diameter.

Experimental Section

Sample Preparation. The arc SWCNTs (Meijo Arc APJ-type, Meijo Nano Carbon, Ltd.) were heated at 350 °C for 30 min in air to remove the most amorphous carbon and other carbon materials, which coat catalyst metal particles. The obtained SWCNTs were treated in a methanol solution of

* Corresponding author. E-mail: toshi.okazaki@aist.go.jp. Phone: +81-29-861-4173. Fax: +81-29-861-6241.
† National Institute of Advanced Industrial Science and Technology.
‡ PRESTO.
§ University of Tsukuba and CREST.
|| Current address: K. K. Air Liquide Laboratories, Tsukuba 300-4247, Japan.
⊥ Current address: Graduate School of Engineering, Nagoya Institute of Technology, Nagoya 466-8555, Japan.

10.1021/jp807630z CCC: $40.75
Published on Web 12/19/2008

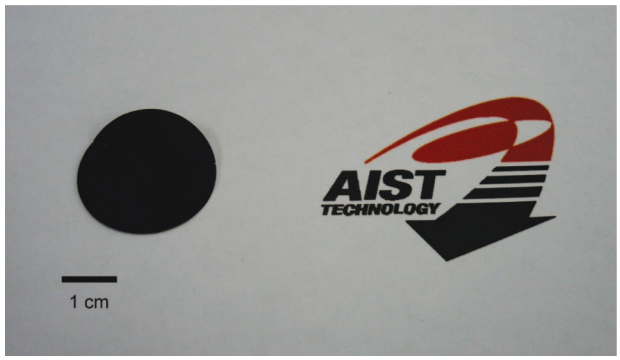

Figure 1. Picture of nanopeapod buckypaper.

sodium hydroxide for 30 min and washed with ethanol several times. Then we washed the remaining metal particles with hydrochloric acid and heated the particles at 600 °C for 2 h in a vacuum. The purity of arc SWCNTs was estimated to be ~90% from the thermogravimetric analysis (TGA) (Supporting Information).

To open the cap of SWCNTs, purified arc SWCNTs were heated at 500 °C for 30 min in air. The treated SWCNTs and fullerenes were sealed under vacuum (~1×10^{-4} Pa) in a quartz tube and then heated at 600 °C for 24 h. The obtained nanopeapods were washed with toluene to remove the fullerenes adsorbed on the outside of the walls. After the filtration, we obtained a dark, paper-like sheet, so-called buckypaper (Figure 1). Without the purification process, the filling yield is very low. For example, if we used raw arc SWCNTs as templates for nanopeapods, we cannot observe any PL peak shifts, even after the C_{60} filling procedure. This means that the filling yield is less than our experimental accuracy of PL measurements (<10%).

For PL measurements, micellar solutions of nanopeapods and SWCNTs were prepared. Briefly, nanopeapods or SWCNTs (~1 mg) were dispersed for 10 min in ~20 mL of D_2O containing 1 wt% of dodecylbenzene sulfonate (SDBS) using a 200 W homogenizer (Sonics VCX500) equipped with a titanium alloy tip (TI-6AL-4V). Each solution was then centrifuged at 127600*g* for 2.5 h (Hitachi CP 100MX), and the supernatant of the upper ~2/3 volume was used.

Characterization. Transmission electron microscope (TEM) images of C_{60} nanopeapods were observed with JEOL JEM-1010 microscopes. PL mapping was performed with a Shimadzu NIR-PL system utilizing an IR-enhanced InGaAs detector (Princeton instruments OMA-V2.2) for detection and a tunable Ti-sapphire laser (Spectra Physics 3900S) for excitation. The slit width for emission was 10 nm. Typical scan steps were 5 and 2 nm for excitation and emission, respectively. The raw data were corrected for wavelength-dependent instrumental factors and excitation laser intensities.

Results and Discussion

TEM Observations. Figure 2 shows typical transmission electron microscope (TEM) images of the produced nanopeapods (Figure 2a−c), together with a reference image of SWCNTs before filling (Figure 2d). The TEM images clearly show that C_{60} fullerenes are highly packed inside the SWCNTs, even in the tip of the tubes (Figure 2b).

PLE Measurements. Figure 3a shows a two-dimensional (2D) PL contour plot of the unfilled arc SWCNTs in SDBS−D_2O solution as a function of emission (λ_{11}) and excitation (λ_{22}) wavelengths. The PL peaks on the map are

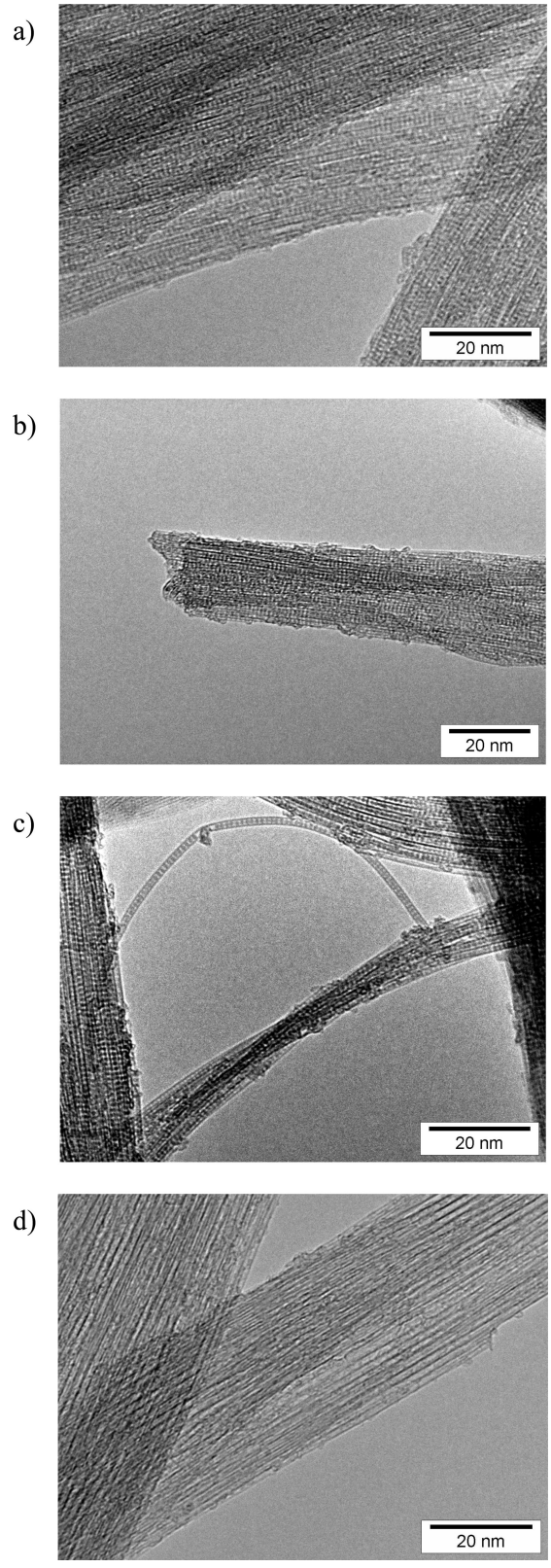

Figure 2. (a−c) Typical transmission electron microscope (TEM) images of the produced nanopeapods. (d) SWCNTs before filling.

clearly seen in the second interband (E_{22}) excitation region (λ_{22} = 870−1070 nm) and the first interband (E_{11}) emission region (λ_{11} = 1500−1800 nm) of SWCNTs with ~1.3−1.5 nm in diameter, which can be assigned to the specific (n, m) SWCNTs by using the empirical relations of Weisman et al.[8] The well-known "$2n + m$" family pattern of SWCNTs is clearly seen in Figure 3a in which the PL peaks with the same $2n + m$ values

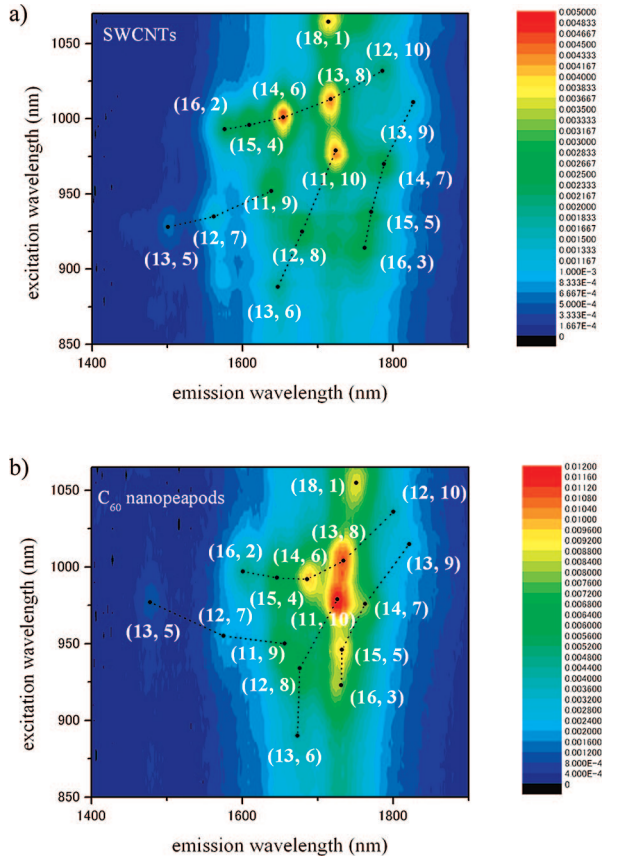

Figure 3. 2D PLE contour plots of (a) SWCNTs and (b) the corresponding C_{60} nanopeapods in SDBS−D_2O solutions.

(similar d_t) are connected.[5,6,9] In the case of the PL peak at $\lambda_{11} \approx 1714$ nm and $\lambda_{22} \approx 1064$ nm, there are no other family members in the PLE map. We assign this peak to the (18, 1) tube because the emission wavelength locates between the (14, 6) and the (13, 8) tubes.[8]

On the other hand, Figure 3b shows the 2D PLE map of C_{60} nanopeapods. A totally different PLE pattern is evidence for the high-yield encapsulations. The $2n + m$ family pattern can also be observed in nanopeapods because the optical band gap shift is expected to be ∼20 meV for SWCNTs with $d_t > 1.3$ nm, which is less than 3% of the original optical band gap.[6] Therefore, the PL peaks can be attributed to each (n, m) nanopeapod as shown in Figure 3b by considering the family pattern. The obtained PL peak positions of SWCNTs and C_{60} nanopeapods in SDBS−D_2O solutions are summarized in Table 1.

Band Gap Modification Mechanisms. In order to investigate the detailed mechanisms of band gap modification, the energy differences in E_{11} and E_{22} between C_{60} nanopeapods and SWCNTs ($\Delta E_{ii} = E_{ii}^{\text{nanopeapods}} - E_{ii}^{\text{SWCNTs}}$, $i = 1, 2$) are plotted as a function of tube diameter (Figure 4a,b). The ΔE_{11} and ΔE_{22} values for smaller diameter nanopeapods are also plotted in panels a and b of Figure 4 by using previous data ($d_t \lesssim 1.3$ nm).[6] Apparently, the diameter dependencies of ΔE_{11} and ΔE_{22} are different between type I and type II tubes. For example, ΔE_{11} for type I tubes shows positive values in a smaller diameter regime. As tube diameter increases, ΔE_{11} exponentially decreases toward −0.02 eV and approaches zero. On the other hand, ΔE_{11} for type II tubes increases toward 0.02 eV as d_t increases and then gradually decreases again (Figure 4a). As is the case of ΔE_{11}, ΔE_{22} also shows clear family type dependence (Figure 4b). Namely, ΔE_{22} for type I tubes increases with increasing tube diameter and then decreases at $d_t \approx 1.4$ nm, whereas ΔE_{22} for type II tubes exhibits a totally opposite trend (Figure 4b).

Such a strong dependence on the $2n + m$ family type is a characteristic feature of the strain-induced spectral shift.[9] Theoretical calculations predicted that the band gaps of E_{11} and E_{22} change in opposite directions of each other upon the structural deformation of SWCNTs caused by the strain.[10] Furthermore, the strain-induced band gap shifts for type I tubes are entirely contrary to those of type II tubes. For example, E_{11} of type I tubes increases under a radial expansion and/or a compressive strain along the tube, whereas that of type II tubes decreases.[10] The observed ΔE_{11} and ΔE_{22} for smaller diameter tubes ($d_t \lesssim 1.32$ nm) correspond to this situation (Figure 4a,b). Tube diameter expansion due to the fullerene encapsulation is responsible for the observed PL peak shifts.[6]

As tube diameter increases, ΔE_{11} and ΔE_{22} approach the zero line and change their signs (Figure 4a,b). Okada and co-workers predicted that C_{60} molecules can enter the interior space of SWCNTs without friction at $d_t \gtrsim 1.3$ nm.[11−13] The diameters of the SWCNTs are unchanged upon fullerene insertion within the calculation accuracy of ∼0.001 nm. In this diameter region, efficient coupling (hybridization) between the π states of C_{60} and the nearly free electron (NFE) states of SWCNTs occurs.[11−13] Electrons are transferred from π orbitals of SWCNTs and C_{60} to the space between them, so that π electron clouds around the nanotube walls expand to the inner and outer spaces.[11−13] Indeed, electron density in the vicinity of the tube wall is found to decrease because of the expansion of the electron clouds for C_{60}@(11, 11) nanopeapods (∼0.05e) ($d_t = 1.48$ nm).[13] The expansion of the electron clouds results in the increase of the resonance integral between the neighboring atoms. Because the π states of SWCNTs and C_{60} radially overlapped in nanopeapods, the resonance integral increases around the circumference of the tube rather than along the tube axis. Such an increase of the resonance integral should cause the same effect as the decrease of the C−C bond length and the corresponding reduction of the effective tube diameter. As a result, the band gap of SWCNTs changes in a family type-dependent manner ($\Delta E_{11} < 0$ and $\Delta E_{22} > 0$ for type I and $\Delta E_{11} > 0$ and $\Delta E_{22} < 0$ for type II) even though the positions of the carbon atoms are unchanged.

The size of the hybridization effects observed here can be estimated as follows. The energy gap change (ΔE_{gap}) between the first van Hove singularities under the uniaxial stress can be expressed as

$$\Delta E_{\text{gap}} = -\text{sgn}(2p+1)3t_0(1+\nu)\sigma\cos 3\theta \qquad (1)$$

where $p = \text{mod}(n - m, 3)$, t_0 is the hopping parameter, ν is Poisson's ratio, and σ is the radial compression and/or the tube elongation.[10] Taking $t_0 = 2.66$ eV and $\nu = 0.2$,[10] we obtain $\sigma = 0.1-0.4\%$ for reproducing the observed ΔE_{11} of the nanopeapods with $d_t \gtrsim 1.32$ nm ($\Delta E_{11} = -4$ to -17 meV for type I and 1−16 meV for type II). This estimation suggests that the hybridization of the π states causes the same effects as the $\sigma = 0.1-0.4\%$ radial compression, which corresponds to the 0.001−0.006 nm reduction of the tube diameter.[6,10]

The computational analysis also predicted that there is an optimum tube diameter in which the space between C_{60} and SWCNTs enhances the hybridization most effectively.[11,12] In our cases, the diameter of ∼1.4 nm is presumably the optimum diameter, which is close to the theoretical predicted value (∼1.5 nm). Naturally, the interaction between C_{60} and SWCNTs becomes weaker as the interwall distance increases between

TABLE 1: Optical Transition Energies of SWCNTs and C_{60} Nanopeapods in SDBS−D_2O and Energy Differences between Them ($\Delta E_{ii} = E_{ii}^{\text{nanopeapods}} - E_{ii}^{\text{SWCNTs}}$, $i = 1, 2$)

		SWCNTs		C_{60} nanopeapods		energy differences	
	(n, m)	E_{11} (eV)	E_{22} (eV)	E_{11} (eV)	E_{22} (eV)	ΔE_{11} (meV)	ΔE_{22} (meV)
type I	(13, 5)	0.825	1.334	0.838	1.268	13	−66
	(12, 7)	0.793	1.325	0.787	1.298	−6	−27
	(16, 2)	0.787	1.246	0.774	1.242	−13	−4
	(11, 9)	0.757	1.301	0.750	1.303	−7	2
	(15, 4)	0.770	1.244	0.753	1.249	−17	5
	(14, 6)	0.750	1.237	0.735	1.249	−15	12
	(13, 8)	0.722	1.224	0.715	1.233	−7	9
	(18, 1)	0.723	1.164	0.707	1.176	−16	12
	(12, 10)	0.693	1.202	0.689	1.197	−4	−5
type II	(13, 6)	0.753	1.396	0.741	1.395	−12	−1
	(12, 8)	0.738	1.337	0.740	1.328	2	−9
	(16, 3)	0.705	1.360	0.719	1.347	13	−14
	(15, 5)	0.701	1.322	0.716	1.309	15	−13
	(11, 10)	0.718	1.268	0.718	1.268	0	0
	(14, 7)	0.693	1.278	0.703	1.271	10	−7
	(13, 9)	0.678	1.226	0.681	1.221	3	−5

them.[10] This tendency can be seen in the diameters beyond 1.5 nm, in which ΔE_{11} and ΔE_{22} approach zero lines (Figure 4a,b).

It is generally accepted that the PL behaviors of SWCNTs are dominated by the Coulomb interaction between the produced electron−hole pairs (excitons). For example, although the one-electron theory predicts that the energy ratio between E_{22} and E_{11} (E_{22}/E_{11}) must approach 2 as tube diameter increases, experimental results show that it approaches a value smaller than 2. This "ratio problem" can be explained by the strong exciton effects in SWCNTs.[14] Figure 5 shows the obtained E_{22}/E_{11} values of C_{60} nanopeapods and SWCNTs as a function of tube diameter. The experimental error for E_{22}/E_{11} is less than 0.01. Interestingly, both E_{22}/E_{11} values approach almost the same value (∼1.75, solid line). This strongly suggests the exciton effects are very similar between SWCNTs and nanopeapods.

It should be noted that such strong diameter and family type dependences in the band gap shifts are distinctive of fullerene nanopeapods. Previously, Li et al. studied the modification of the band gap structure of SWCNTs by the encapsulation of manganese ditelluride ($MnTe_2$).[15] Almost uniform red shifts in both excitation and emission wavelengths in the PLE map were observed upon $MnTe_2$ encapsulations, which is explained by the local environment change rather than the structural deformation of SWCNTs. To elucidate a general rule for the band gap engineering of SWCNTs, further investigation is necessary for SWCNTs encapsulating various organic and inorganic materials.

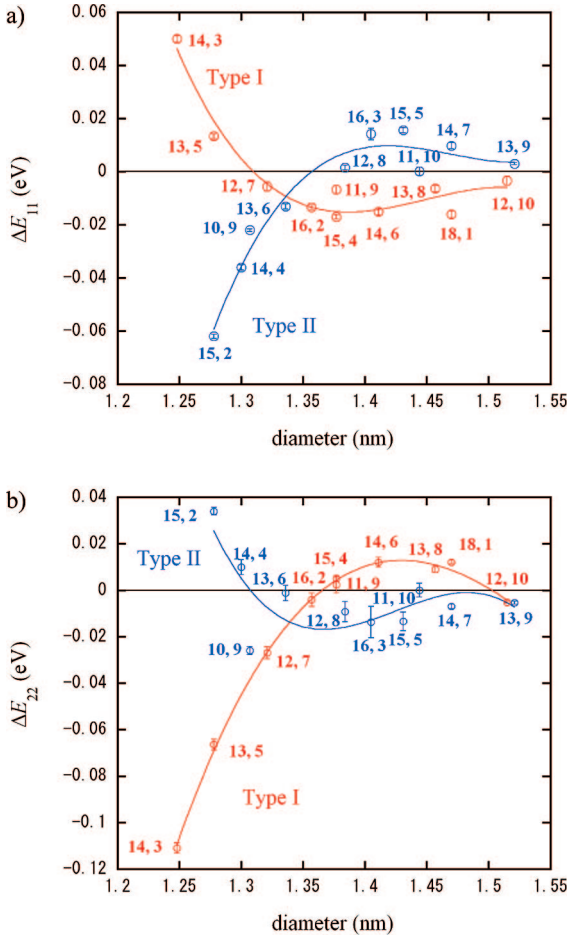

Figure 4. Differences in optical transition energies in (a) E_{11} and (b) E_{22} (ΔE_{11} and ΔE_{22}, respectively) between C_{60} nanopeapods and SWCNTs as a function of tube diameter.

Conclusions

In summary, PL behaviors of C_{60} nanopeapods were investigated over a wide range of diameters. PLE results reveal the

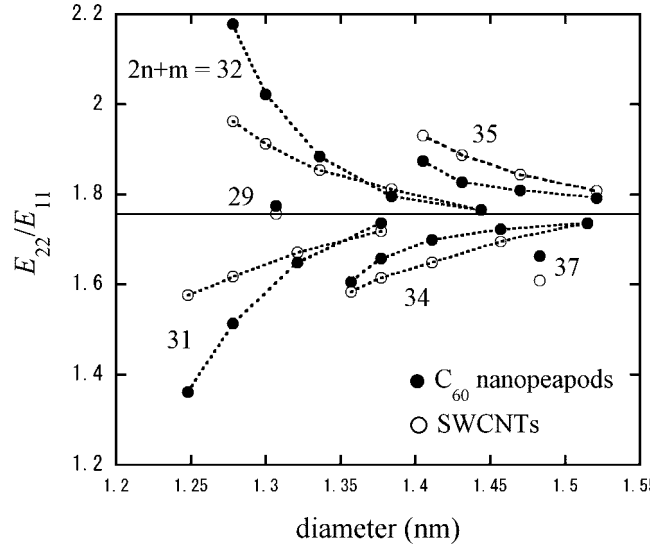

Figure 5. E_{22}/E_{11} for SWCNTs and nanopeapods as a function of tube diameter.

characteristic band gap shifts of SWCNTs upon C_{60} encapsulation. For nanopeapods with smaller diameters ($d_t \lesssim 1.32$ nm), the band gap of SWCNTs is modified by the mechanical strain because of encapsulated C_{60}. For larger diameter regimes ($d_t \gtrsim 1.32$ nm), hybridization between the π state of C_{60} and the NFE state of SWCNTs induces the same effects as the small reduction of the tube diameter, resulting in the family type-dependent band gap shifts.

Acknowledgment. The authors thank Dr. T. Saito (National Institute of Advanced Industrial Science and Technology) for his experimental help. A part of this work is supported by the NEDO Nano-Carbon Technology project.

Supporting Information Available: TGA and the resonant Raman spectrum of purified Arc SWCNTs. This material is available free of charge via the Internet at http://pubs.acs.org.

References and Notes

(1) Britz, D. A.; Khlobystov, A. N. *Chem. Soc. Rev.* **2006**, *35*, 637–659.

(2) Okazaki, T.; Shinohara, H. In *Applied Physics of Nanotubes: Fundamentals of Theory, Optics, and Transport Devices*; Rotkin, S. V., Subramoney, S., Eds.; Springer: Berlin, 2005; Chapter 5.

(3) (a) Lee, J.; Kim, H.; Kahng, S.-J.; Kim, G.; Son, Y.-W.; Ihm, J.; Kato, H.; Wang, Z. W.; Okazaki, T.; Shinohara, H.; Kuk, Y. *Nature* **2002**, *415*, 1005–1008. (b) Hornbaker, D. J.; Kahng, S.-J.; Misra, S.; Smith, B. W.; Johnson, A. T.; Mele, E. J.; Luzzi, D. E.; Yazdani, A. *Science* **2002**, *295*, 828–831.

(4) Shimada, T.; Okazaki, T.; Taniguchi, R.; Sugai, T.; Shinohara, H.; Suenaga, K.; Ohno, Y.; Mizuno, S.; Kishimoto, S.; Mizutani, T. *Appl. Phys. Lett.* **2002**, *81*, 4067–4069.

(5) Weisman, R. B. In *Applied Physics of Carbon Nanotubes: Fundamentals of Theory, Optics, and Transport Devices*; Rotkin, S. V., Subramoney, S., Eds.; Springer: Berlin, 2005; pp 183−202.

(6) Okazaki, T.; Okubo, S.; Nakanishi, T.; Joung, S.-K.; Saito, T.; Otani, M.; Okada, S.; Bandow, S.; Iijima, S. *J. Am. Chem. Soc.* **2008**, *130*, 4122–4128.

(7) Okazaki, T.; Saito, T.; Matsuura, K.; Ohshima, S.; Yumura, M.; Oyama, Y.; Saito, R.; Iijima, S. *Chem. Phys. Lett.* **2006**, *420*, 286–290.

(8) Weisman, R. B.; Bachilo, S. M. *Nano Lett.* **2003**, *3*, 1235–1238.

(9) Jorio, A.; Fantini, C.; Pimenta, M. A.; Capaz, R. B.; Samsonidze, G. G.; Dresselhaus, G.; Dresselhaus, M. S.; Jiang, J.; Kobayashi, N.; Grüneis, A.; Saito, R. *Phys. Rev. B* **2005**, *71*, 075401.

(10) Yang, L.; Han, J. *Phys. Rev. Lett.* **2000**, *85*, 154–157.

(11) Otani, M.; Okada, S.; Oshiyama, A. *Phys. Rev. B* **2003**, *68*, 125424.

(12) Okada, S.; Saito, S.; Oshiyama, A. *Phys. Rev. Lett.* **2001**, *86*, 3835–3838.

(13) Okada, S. *Chem. Phys. Lett.* **2007**, *438*, 59–62.

(14) Kane, C. L.; Mele, E. J. *Phys. Rev. Lett.* **2003**, *90*, 207401.

(15) Li, L.-J.; Lin, T.-W.; Doig, J.; Mortimer, I. B.; Wiltshire, J. G.; Taylor, R. A.; Sloan, J.; Green, M. L. H.; Nicholas, R. J. *Phys. Rev. B* **2006**, *74*, 245418.

JP807630Z